Comparison of ROI quantification for three PET reconstruction methods

J.B. Moody[1], B.C. Lee[1], E.P. Ficaro[1,2]

1. INVIA Medical Imaging Solutions, Ann Arbor, Michigan
2. University of Michigan, Dept. of Radiology, Ann Arbor, Michigan

University of Michigan Health System

INVIA Medical Imaging Solutions

OBJECTIVE

To evaluate ROI quantification for three types of PET reconstruction methods: standard OSEM, penalized weighted least-squares with quadratic penalty (PWLSQuad), and the wavelet-based iterative shrinkage-thresholding (IST) method.

INTRODUCTION

In order to optimize ROI quantification accuracy and precision, PET image reconstruction methods must be able to control bias and variance within the ROI. A recent publication [1] has shown that in general the optimal bias-variance trade off will depend on lesion size and lesion-to-background contrast. In this poster, we vary lesion size, keeping contrast fixed. OSEM is the only method currently in clinical use that allows some control over bias-variance (e.g. by number of iterations and post-filtering). Quadratic PWLS is the state-of-the-art but not widely used clinically due to the difficulty selecting an optimal hyperparameter β. Recently it was suggested that the quadratic penalty sets a bound on the lowest bias-variance that can be achieved among `edge-preserving' penalties[2]. IST is a more recent method that uses a sparse image representation (in the wavelet domain) combined with an L1 penalty term.

METHODS

PET Simulations

- A digital NEMA NU2-2001 phantom was used with six spheres of diameter: 10, 13, 17, 22, 28, 37 mm, and 4:1 sphere-to-background activity concentration ratio and 128x128 matrix size.
- Sinograms were simulated analytically with attenuation, non-uniform detector efficiency, random coincidences (10%) and Poisson noise with approximately 2×10^6 total counts.
- 200 noise realizations were generated and each simulated sinogram reconstructed by all methods.

Image Analysis

- Reconstructed sphere activity was quantified using the known sphere boundaries.
- Global and per-sphere RMS error and bias-variance tradeoff curves were computed per sphere.

Reconstruction methods

- The OSEM method used 6 subsets, 5 iterations and post-smoothing with 6mm FWHM Gaussian kernel, which gave the lowest global RMSE for the simulated images.
- The PWLS method was implemented using a block iterative separable paraboloidal surrogates algorithm[3] with 6 subsets and 150 iterations to ensure full convergence.
- The IST reconstruction method[4,5] was implemented for emission reconstruction with the dual-tree complex wavelet transform (right) [6], 4 decomposition levels, and three different thresholding approaches:
  - soft thresholding with global threshold (*DT-CWT*) [5].
  - soft thresholding with a local adaptive threshold (*DT-CWT-SoftAdapt*).
  - bivariate shrinkage accounting for interscale dependencies between wavelet coefficients (*DT-CWT-BivSh*) [6].

RESULTS

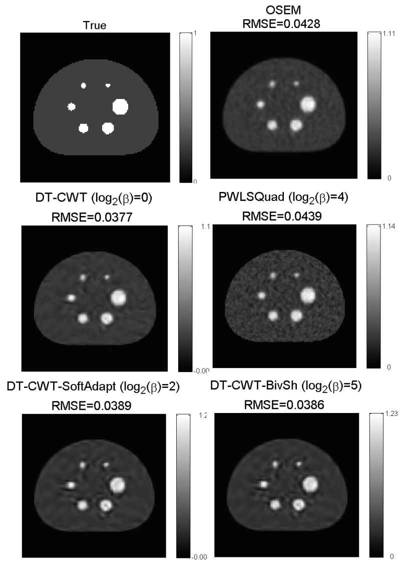

True image (upper left) and reconstructed images for all methods with the corresponding β value yielding the lowest global RMS error in each case.

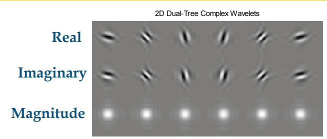

Basis elements of the dual-tree CWT used for IST methods. The real and imaginary parts are oriented at ±75°, ±45°, and ±15°, and the magnitudes are isotropic and approximately shift invariant.

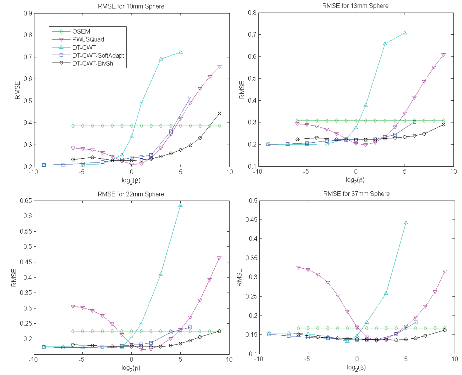

RMSE per sphere as a function of regularization parameter β. The optimal β for PWLSQuad varies with sphere size. However, for the IST methods RMSE is remarkably constant over a broad range of β values.

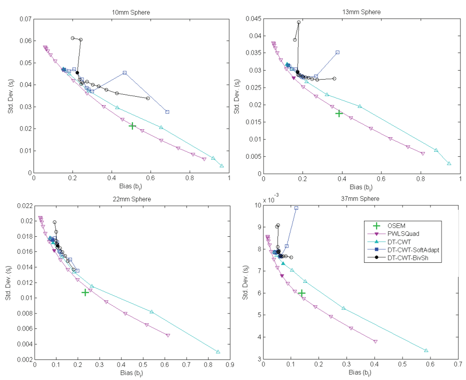

Bias-variance trade-off curves (parameterized by β). For IST methods the trade-off was either similar to PWLSQuad (DT-CWT), or more concentrated near the optimal β for PWLSQuad (DT-CWT-SoftAdapt, DT-CWT-BivSh). However, per sphere bias-variance for PWLSQuad appeared to give a lower bound for all methods considered.

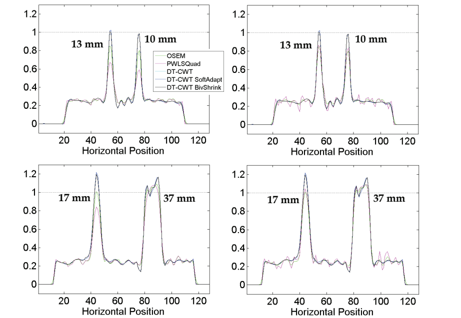

Horizontal profiles through centers of 10, 13 mm spheres (upper) and 17, 37 mm spheres (lower). A single β value was used for each IST method. All three IST methods show good count recovery simultaneously with smooth background. For PWLSQuad two different β values were needed to approximately match overall IST variance (left) and IST count recovery within spheres (right).

CONCLUSIONS

- IST methods achieved the lowest global RMS error, about 9-11% lower than OSEM, and 11-14% lower than that of PWLSQuad.
- For fixed iteration number, OSEM per-sphere RMS error increased with decreasing sphere diameter.
- IST methods had remarkably constant per-sphere RMS error over a broad range of β values, which could simplify optimal β selection in clinical applications.
- Lower bounds of bias-variance trade-off for IST methods were close to that of PWLSQuad.
- IST methods showed better count recovery per sphere at high levels of overall smoothing and fixed β.
- IST methods may offer a practical alternative for optimal clinical reconstruction of high count pre-corrected PET data and accurate, robust ROI quantification.
- Future directions:
  - Analyze convergence properties of IST methods
  - Generalize IST to 3-dimensional data
  - Anisotropic wavelet basis, wavelet packets

REFERENCES

[1] J. Qi and H. Huesman, "Theoretical study of penalized-likelihood image reconstruction for region of interest quantification," Medical Imaging, IEEE Transactions on, vol. 25, 2006, pp. 640-648.
[2] J. Qi, "Comparison of Lesion Detection and Quantification in MAP Reconstruction with Gaussian and Non-Gaussian Priors," International Journal of Biomedical Imaging, vol. 2006, 2006.
[3] J. Fessler, "Penalized weighted least-squares image reconstruction for positron emission tomography," Medical Imaging, IEEE Transactions on, vol. 13, 1994, pp. 290-300.
[4] I. Daubechies, M. Defrise, and C.D. Mol, "An iterative thresholding algorithm for linear inverse problems with a sparsity constraint," Comm.Pure Applied Math, vol. 57, 2004, pp. 1413-1457.
[5] J. Zhou, J. Coatrieux, A. Bousse, et al., "A Bayesian MAP-EM Algorithm for PET Image Reconstruction Using Wavelet Transform," Nucl Sc, IEEE Trans, vol. 54, 2007, pp. 1660-1669.
[6] I. Selesnick, R. Baraniuk, and N. Kingsbury, "The dual-tree complex wavelet transform," Signal Processing Magazine, IEEE, vol. 22, 2005, pp. 123-151.